

# Reconstructing Enhanced Resolution Images From Spaceborne Microwave Sensors

Douglas R. Daum, David G. Long, and Warren B. Davis  
Brigham Young University  
Electrical and Computer Engineering Department  
459 Clyde Building, Provo, UT 84602

*Abstract* - Low resolution has limited the land applications of spaceborne microwave remote sensors, particularly radiometers. To overcome this limitation, we apply two image enhancement algorithms to radiometer data for land and ice studies: a modified version of the scatterometer image reconstruction algorithm and the Backus and Gilbert inversion technique. We compare these methods' effectiveness over land and ice areas by imaging radiometric data from the Special Sensor Microwave/Imager (SSM/I) and the Seasat-A Scanning Multichannel Microwave Radiometer (SMMR) as well as the Seasat-A (SASS) and the ERS-1 scatterometer. The image resolution depends on the footprint shape in addition to the footprint size. Inverse filtering improves image quality by compensating for the microwave sensor's intrinsic low pass filtering. We describe methods for developing the inverse filter.

## I. INTRODUCTION

Microwave sensors are a powerful tool in geophysical research due to their ability to penetrate most cloud and atmospheric conditions. Unfortunately, most passive microwave sensors have very low resolution (typically 15 to 100 km). Thus, although microwave radiometers have been carried on spaceborne platforms for over two decades, most studies have been performed over uniform background brightness temperature regions such as the ocean.

To improve the resolution over land masses, we have compared two image reconstruction algorithms. These algorithms offer enhanced resolution by exploiting the data from overlapping antenna patterns. We also filter the images to compensate for the shortcomings of the sensor measurements.

In this paper we: (1) describe the two image reconstruction algorithms, (2) discuss the inverse filtering method, and (3) apply the algorithms to data from SSM/I, SMMR, ERS-1, and SASS.

## II. IMAGE RECONSTRUCTION ALGORITHMS

Before discussing how we achieve high resolution images, we must define the goals of two processes: image reconstruction and image compensation. First, it is the goal of image reconstruction to produce two dimensional images from raw sensor data at enhanced resolution. Image reconstruction algorithms are limited, however, by the sensor's intrinsic low pass filtering of the data. Therefore, image compensation is applied to a reconstructed image to further recover some of the information attenuated by the sensor response. Thus, we first apply an image reconstruction technique to give an enhanced image and then compensate the image using inverse filtering.

Our first reconstruction technique is a variation of the scatterometer image reconstruction (SIR) algorithm (Long et al., 1993). In SIR, a brightness temperature is predicted for each image pixel and then compared to the actual data measurement. New pixel predictions are made by a nonlinear scaling of the previous prediction based on the ratio of the predicted and measured brightnesses. The algorithm is iterated until the scale factor converges to unity and the image pixel values are determined.

Our second reconstruction technique is the Backus-Gilbert (BG) inversion method. This method predicts each pixel value by using a linear combination of measurements near the desired pixel. Subjectively chosen parameters within the algorithm determine the number of the "nearby" measurements for the combination. Other studies have used these parameters to adjust spatial resolution between different microwave channels (Robinson et al., 1992) and to optimally suppress noise (Poe, 1990).

We have investigated the SIR and BG algorithms with the aid of simulated measurements. The synthetic data represented typical brightness temperatures and features over the Amazon Delta. We generated these files at different spatial densities using artificial antenna

patterns similar to those used by spaceborne sensors and qualitatively compared the results.

We found that for densely sampled measurements (a high spatial sampling density), the BG reconstruction provided better edge enhancement than the SIR algorithm. Unfortunately, the BG algorithm also produced more artifacts in the reconstructed image than SIR. For low spatial sampling densities, however, the SIR and BG images had equivalent edge clarity, but SIR did not produce the processing artifacts. In addition, the SIR processing time was approximately 50 times faster than the BG algorithm. As a result, SIR was selected for processing sensor data from SSM/I, SMMR, ERS-1, and SASS.

## III. IMAGE COMPENSATION

The second step in improving resolution is image compensation. Although SIR and BG produce higher resolution images than other conventional methods, the images can be further improved by compensating for the antenna response of the microwave sensor. We have developed an inverse filtering method to achieve this compensation for SIR but have not yet applied it to BG.

To illustrate the image compensation, we determine the SIR-sensor wavenumber response by processing a synthetic circularly symmetric image with a cross section similar to a chirp function and center bright spot approximately the sensor footprint size (see Figure 1). We process the image by applying SIR to samples of the image taken with the same antenna pattern and sampling density as the microwave sensors' data (see Figure 1). Figure 2 shows the cross section of the test and reconstructed images. The difference between the 2D chirp and the reconstructed image suggests the use of an inverse filter as a means to regain part of the lost wavenumber information from the test image. The inverse filter is determined by subtracting the envelope of the SIR reconstructed chirp from the original chirp. This yields a high pass filter since the filter magnitude increases with increasing frequency. The filter, however, is modified to be a bandpass filter so that high frequency noise is not over-amplified. We applied two derived bandpass filters (Figure 3) to generate the filtered images found in Figure 4. The resulting images show improvement on the outer parts of the chirp (high frequency) at a small expense to the center of the chirp (low frequencies). This tradeoff is governed by the cutoff frequency of the filters used.

Further cross sectional wavenumber analysis for other sensors indicates that image resolution depends on footprint orientation as well as size. For example, as described in Davis (1993), the SASS data yields very high resolution images. The higher resolution results from SIR's ability to extract information from the narrow dimension of SASS's very elongated sensor footprints. For example, the upper left corner of Figure 5 (a) illustrates the SASS footprint shape. A "star" like pattern appears when multiple samples are taken at the same location using different orientations (see (b) of Fig. 5). This footprint orientation pattern is also detected in the chirp image reconstruction (Figure 5). Thus, the overlap within this star pattern explains the high resolution enhancement obtained from SASS data (Long et al., 1993).

## IV. SIR APPLIED TO VARIOUS SENSORS

We have applied the SIR algorithm to several sensors including the SSM/I, SMMR, ERS-1, and SASS. Sample SMMR and SSM/I images of Greenland are located at the end of this article (Figs. 6 - 7) while ERS-1 and SASS images are included in Early et al. (1994). The SSM/I images illustrate the tradeoffs between resolution and emission for each microwave frequency. While the higher frequencies have better resolution, they lack the brightness variation from different snow types. The brightness variation in the time series corresponds to the borders of surface snow/ice for the months of July, August, and September 1978.

Further research will compare the 1978 SMMR images directly to the 1992 SSM/I images to investigate decadal changes on the Greenland ice sheets. Image flaws result from data errors.

We have also used the SIR and BG algorithms to reconstruct images of the Amazon Delta. We found that the image brightness temperatures vary spatially according to surface vegetation and temporally according to atmospheric conditions. By combining several reconstructed images from single passes, we remove the temporal atmospheric distortions to generate a brightness background mapping of the region. Since the Amazon has low seasonal variation over short periods of time, this mapping can be used to discriminate between surface vegetation types as in Long et al. (1993). In addition, we can detect atmospheric conditions in other passes by comparing them with the background mapping.

### V. SUMMARY AND CONCLUSIONS

Improved resolution increases the effectiveness of land studies using microwave sensors. This resolution depends on choosing a reconstruction algorithm according to sampling density: SIR for low density and BG for high density. In addition, the resolution may be further enhanced through a compensating inverse filter. This enhancement has been shown both by imaging synthetic as well as real data. Greenland images from microwave sensors illustrate the improved resolution and its use in temporal change studies and multifrequency comparisons.

### REFERENCES

- Davis, W. B. "Enhanced Resolution from Remotely Sensed Microwave Data," Master's Thesis, Brigham Young University, Provo, UT, 1993.
- Early, D. S., D. G. Long, and M. R. Drinkwater, "Comparison of Enhanced Resolution Images of Greenland from the ERS-1 and Seasat Scatterometers," in IGARSS Digest, 1994.
- Long, D. G., D. S. Early, and M. R. Drinkwater, "Enhanced Resolution ERS-1 Scatterometer Imaging of Southern Hemisphere Polar Ice," in IGARSS Digest, 1994.
- Long, D. G., P. J. Hardin, and P. T. Whiting, "Resolution Enhancement of Spaceborne Scatterometer Data," IEEE Trans. on Geosci. and Remote Sens., Vol. 31, No. 3, pp. 700-715, May 1993.
- Poe, G. A., "Optimum Interpolation of Imaging Microwave Radiometer Data," IEEE Trans. on Geosci. and Remote Sens., Vol. 28, No. 5, pp. 800-810, Mar. 1990.
- Robinson, W. D., C. Kummerow, and W. S. Olson, "A Technique for Enhancing and Matching Resolution of Microwave Measurements from the SSM/I Instrument," IEEE Trans. on Geosci. and Remote Sens., Vol. 30, No. 3, pp. 419-429, May 1992.

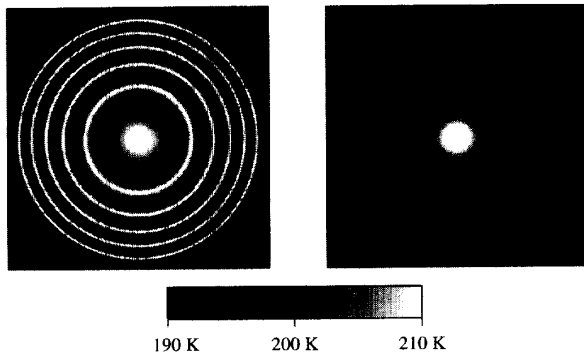


Figure 1  
Test (L) and SIR (R) Image for Simulated 6.6 GHz SMMR Data

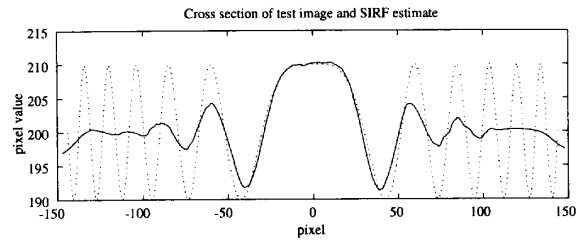


Figure 2  
Cross Section of Test and SIR from 6.6 GHz SMMR Data

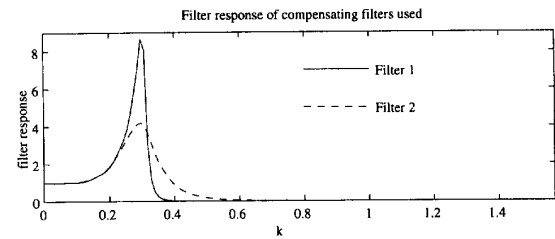


Figure 3  
Filter Response of Two Compensating Filters

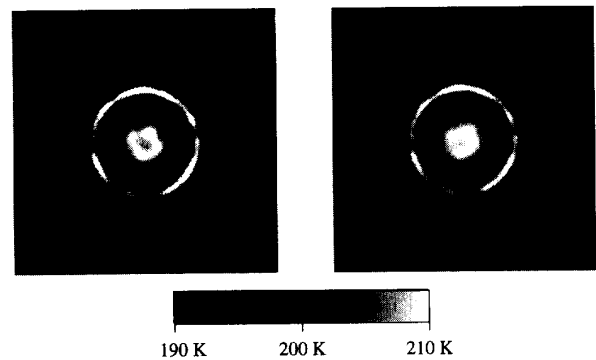


Figure 4  
SIR Images After Compensation by Filter 1 (L) and Filter 2 (R)

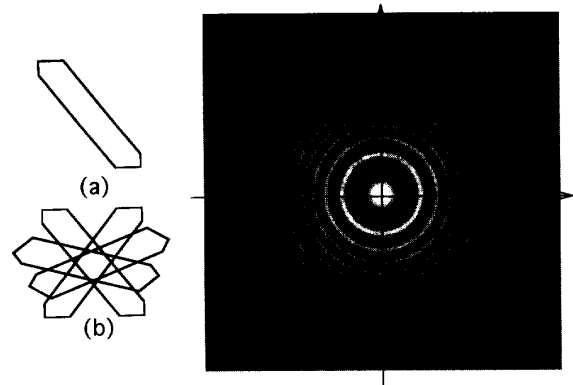


Figure 5  
SASS Footprint Shape (a), Orientations (b), and the Corresponding SIR Test Image from Simulated Data

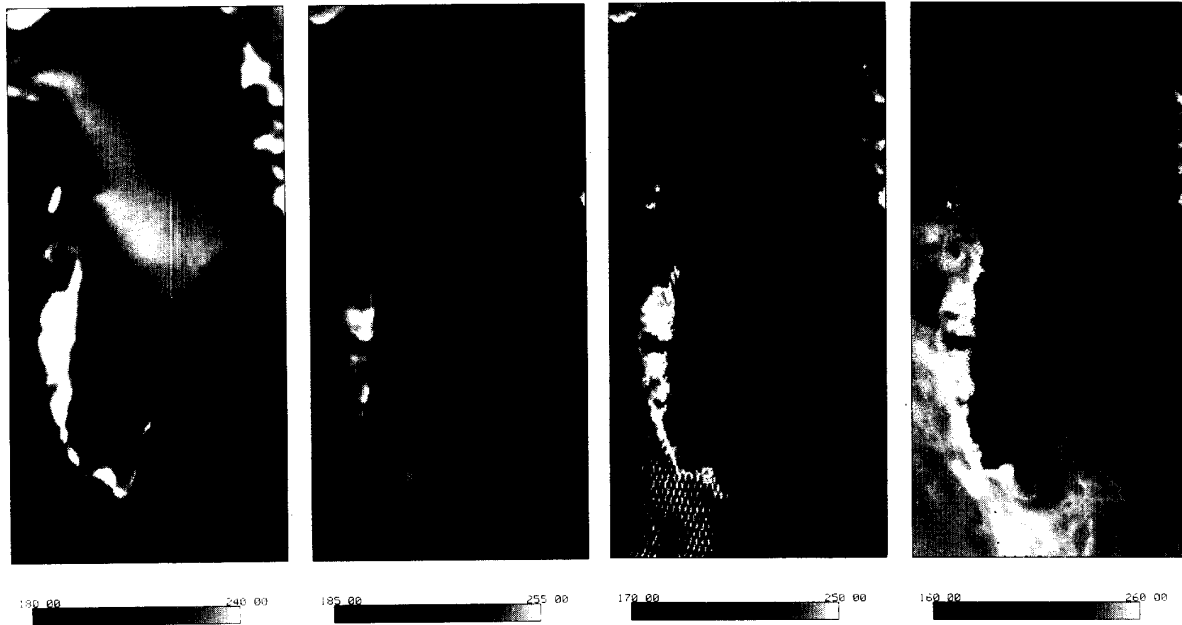


Figure 6  
 SIR SSM/I V-pol Brightness Temperature Images of Greenland, JD 250  
 (left to right 19.35, 22.235, 37.0 and 85.0 GHZ)



Figure 7  
 Time Series SIR SMMR Images of Greenland from Four Day Periods During  
 July, August, and September, 1978  
 (respectively from left to right)